J. Membrane Biol. 180, 195–203 (2001)
DOI: 10.1007/s002320010070

The Journal of
Membrane
Biology

Lipid-induced Pore Formation of the *Bacillus thuringiensis* Cry1Aa Insecticidal Toxin

V. Vié[1]*, N. Van Mau[2]*, P. Pomarède[3], C. Dance[3], J.L. Schwartz[4,5], R. Laprade[4], R. Frutos[3], C. Rang[3], L. Masson[5], F. Heitz[2], C. Le Grimellec[1]

[1]CBS, 29 rue de Navacelles, 34090 Montpellier Cedex, France
[2]CRBM, CNRS-UPR 1086, 1919 route de Mende, 34293 Montpellier Cedex 5, France
[3]CIRAD, Avenue Agropolis, BP 5035, 34032 Montpellier Cedex 1, France
[4]Groupe de Recherche en Transport Membranaire, Université de Montréal, Montréal, Quebec H3C 2J7, Canada
[5]Biotechnology Research Institute, 6100 Royalmount Avenue, Montréal, Quebec H4P 2R2, Canada

Received: 14 July 2000/Revised: 28 December 2000

Abstract. After activation, *Bacillus thuringiensis* (Bt) insecticidal toxin forms pores in larval midgut epithelial cell membranes, leading to host death. Although the crystal structure of the soluble form of Cry1Aa has been determined, the conformation of the pores and the mechanism of toxin interaction with and insertion into membranes are still not clear. Here we show that Cry1Aa spontaneously inserts into lipid mono- and bilayer membranes of appropriate compositions. Fourier Transform InfraRed spectroscopy (FTIR) indicates that insertion is accompanied by conformational changes characterized mainly by an unfolding of the β-sheet domains. Moreover, Atomic Force Microscopy (AFM) imaging strongly suggests that the pores are composed of four subunits surrounding a 1.5 nm diameter central depression.

Key words: Lipid monolayers — Protein insertion — Cry1Aa toxin — Amphipathic properties — Pore formation

Introduction

Bacillus thuringiensis (Bt) insecticidal toxins are currently the focus of a worldwide debate on the agricultural impact of transgenic plants, including insect resistance and nontarget effects. For example, it has been reported that some insects evolve resistance to Bt (Tabashnik et al., 1997) and that, due to its presence in corn pollen, Bt is potentially dangerous for the conservation of monarch butterflies (Losey, Rayor & Carter, 1999). The toxicity is thought to be induced by binding to specific target sites in the midgut brush border, creating pores that disrupt the ionic balance and thus kill the insect. Although various reports on Bt resistance have demonstrated altered receptor binding patterns, numerous cases have shown normal binding (Schnepf et al., 1998) thus implicating the involvement of post-binding events like pore formation, the mechanisms of which are largely unknown. Although the Cry1Aa toxin atomic structure (Grochulski et al., 1995) has been delineated, models describing membrane permeation by toxin and/or pore structures in lipid bilayers are still only based on indirect data derived from genetic, fluorescent and planar lipid bilayer studies (Schwartz et al., 1993; Gazit & Shai, 1995; Schwartz et al., 1997; Gazit et al., 1998; Masson et al., 1999). These latter showed that the presence of receptor is not a prerequisite for pore formation and proposed a model that is based on a tetrameric association of the toxin leading to an aggregate so that the hydrophilic faces of four α4 helices form the lumen of the pore.

To understand the mechanism by which the toxin can spontaneously insert into certain membranes (Masson et al., 1999) leading the formation of an ion channel even in the absence a receptor; we decided to study the interactions of the toxin with lipids using the monolayer approach (Brockman, 1999). Further, protein-containing monolayers were transferred for AFM observations with the aim of identification of the topological organization of the protein and thus of the nature of the particle giving rise to pore formation that will be analyzed in connection with FTIR observations. We describe here the adsorp-

Correspondence to: F. Heitz

* Both authors contributed equally to this work.

tion properties of the Cry1Aa toxin at an air-water interface in the presence or absence of lipids, together with the AFM imaging of the protein when engaged in a monolayer and a bilayer. The consequences of the conformational changes detected by FTIR are discussed in association with the AFM images obtained on mono- and bilayers, respectively.

Materials and Methods

Materials

Natural heart bovine phosphatidylethanolamine (PE) and phosphatidylcholine (PC), and synthetic dipalmitoylphosphatidylethanolamine (DPPE), dipalmitoylphosphatidylcholine (DPPC), dioleoylphosphatidylethanolamine (DOPC) and dipalmitoylphosphatidylglycerol (DPPG) were purchased from Avanti Polar Lipids (Alabaster, AL, USA). Cholesterol (CH) was purchased from Sigma (St Louis, MO, USA). Organic solvents were obtained from Merck (Darmstadt, Germany) and water was tridistilled (once on MnO_4K).

Toxin Preparation

Production and purification of the recombinant Cry1Aa *B. thuringiensis* toxin by trypsin activation was conducted as described elsewhere (Rang et al., 1999). Purified toxin was dialyzed for 48 hr at 4°C against 20 mM Tris-HCl pH 8.6, quantified (Bradford, 1976) and diluted to 260 ng/ml in 20 mM Tris-HCl pH 8.6, then lyophilized and stored at −80°C. Prior to the dilution process, we verified by dynamic light scattering that the toxin was in a monomeric state in the parent solution (i.e, 0.26 mg/ml).

Measurements at the Air-Water Interface

The toxin was allowed to adsorb at the air-water interface. Variations in surface tension upon increasing the protein concentration into the subphase (pH 9.34, which corresponds to the pH of insectidal midguts, and which is required for protein activation) was measured with a platinum plate by the Wilhelmy plate methods as previously described (Van Mau et al., 1999), using a rectangular teflon trough (120 × 70 mm), 5 mm depth, a Prolabo tensiometer (Paris, France) and a Kipp and Zonen (Delft, The Netherlands) X-Y recorder, model BD 91.

The ability of the toxin to insert into lipids was determined by measuring increases in surface pressure of spread lipid monolayers (*see* Results and Discussion and Table for compositions) at various initial pressures upon injecting an aqueous toxin solution in the subphase (5×10^{-8} M).

Protein-lipid interactions for various lipid compositions of the monolayers (*see* Table) were achieved using an initial lipid surface pressure close to that obtained for the pure protein at saturation (23 mN/m) (Rafalski, Lear & DeGrado, 1990). The solution was gently stirred with a magnetic stirrer and equilibrium was obtained after 3–5 hr depending on the components of the monolayer. All of the system was maintained under an argon atmosphere to avoid lipid oxidation.

Langmuir-Blodgett Transfers

Langmuir-Blodgett (LB) transfers of monolayers were achieved as previously described (Vié et al., 1998; Van Mau et al., 1999). Aliquots of a lipidic solution in a chloroform-methanol (3:1, v/v) volatile solvent were spread on a 0.1 M sodium carbonate buffer (pH 9.34) contained in a teflon trough (dimensions 90 × 140 mm with a central 15 mm deep hole for accommodation of the support). After complete solvent evaporation, the lipid monolayer was compressed with a hydrophobic barrier to the selected surface pressure (24 mN/m). The toxin was injected into the subphase (5×10^{-8} M) and the transfer was performed after the surface tension had reached equilibrium (30 mN/m). This transfer procedure was achieved by raising the solid support (freshly cleaved mica) immersed in the liquid through the monolayer while surface pressure was kept constant by a feedback system (Van Mau et al., 1999). To transfer bilayers, a monolayer of pure DPPC was first transferred as described above. Another lipid film was then spread and compressed to the surface pressure selected. The protein was allowed to penetrate the lipid film and the second layer was obtained by pulling down the hydrophobic support through the mixed protein-lipid monolayer at constant surface pressure. The hydrophilic sample obtained was maintained in the buffered solution until the AFM imaging has been performed.

Atomic Force Microscopy Imaging

AFM imaging of LB films was performed with a Nanoscope III atomic force microscope from Digital Instruments (Santa Barbara, CA, USA) under ambient conditions, equipped with a 14 m scanner. Monolayers were imaged in air and bilayers were imaged in the buffer solution. Topographic images were acquired in constant force mode, using silicon nitride tips on integral cantilevers with a nominal spring constant of 0.06 N/m (Le Grimellec et al., 1994). Applied force during scanning in liquid was maintained below 200 pN (Müller, Büldt & Engel, 1995; Le Grimellec et al., 1998). The scan rate varied from 2–5 Hz, according to the scan range.

FTIR Measurements

FTIR spectra were obtained on a Bruker IFS 28 (Wissembourg, France) spectrophotometer. The spectra (500 scans) were recorded on samples that were prepared by depositing solutions of lipids (DPPG or DPPC/DOPE/CH (5/4/1, mole/mole)) and of the protein onto fluorine plates and allowing the solvents to evaporate under a nitrogen flux. Spectra in solution were recorded using a horizontal germanium ATR plate. Spectra analyses were performed using the OPUS (Bruker) software.

Results and Discussion

Amphipathic Character of Cry1Aa

Lipid-free Air-Water Interface

As a prerequisite for the study of Cry1Aa insertion into membranes using the monolayer approach, we first examined the adsorption of the protein at a lipid-free air-water interface, in order to define the experimental conditions for penetration and evidence the amphipathic properties of Cry1Aa in an anisotropic surface environment (Grochulski et al., 1995). Using a 0.1 M carbonate buffer solution (pH 9.3, close to the pH of insect midguts required to solubilize the protein) (Masson et al., 1999)

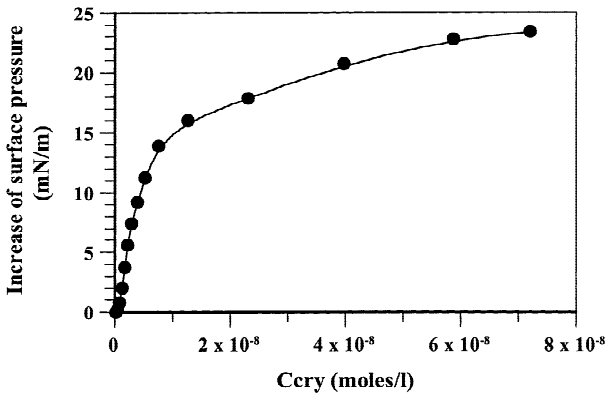

Fig. 1. Variation of the surface pressure upon adsorption of Cry 1A molecules at the air-water interface. Increasing concentrations of Cry1Aa were injected into the aqueous phase.

as subphase, Cry1Aa was injected progressively in the bulk and allowed to adsorb at the air-water interface. The surface pressure at saturation was found to be relatively high (25 mN/m; Fig. 1) indicating that, in accordance with the X-ray data, the toxin has a strong amphipathic character (Grochulski et al., 1995) with formation of oligomers, as recently reported from size-exclusion chromatography experiments (Güereca & Bravo, 1999). The formation of such a species requires at least a partial unfolding of the protein facilitating hydrophobic interactions leading to the oligomerization. Such an unfolding is a phenomenon that occurs when a protein is engaged in an anisotropic interface as is the case for an air-water interface (Green, Hopkinson & Jones, 1999). In the last highest concentration range, the balanced ratio between hydrophobic and hydrophilic parts of adsorbed oligomers forms an orientated monolayer with the polar heads anchored in the aqueous solution. Thus, the surface pressure that is measured results from both hydrophobic and electrostatic interactions. The amphipathic character of the protein demonstrated in this work is an important property required for an adsorption at the lipid monolayer/aqueous solution interface.

Lipid-containing Air-Water Interface

To analyze the membrane insertion process we compared the interactions of Cry1Aa with pure lipids where the physical state and polar headgroups have been varied. On the basis of the experiments carried out in the lipid-free conditions, the initial pressure of the lipid monolayer was set at 23 mN/m for all experiments, a value that approximates the maximum pressure obtained without lipid. These conditions allowed us to assign the changes of the surface pressure upon addition of the protein (5×10^{-8} M) to the interactions between the protein and the lipid(s) (Rafalski, Lear & DeGrado, 1990). For monolayers made of single phospholipid species, dipalmitoylphosphatidylethanolamine (DPPE) or dioleoylphosphatidyl-ethanolamine (DOPE), comparison of the Cry1Aa-induced variations of surface pressures indicated that the protein-lipid interactions were favored when the lipid is in the liquid condensed state (DPPE) rather than in the liquid expanded state (DOPE) (Table). This difference could have its origin in the hydrophobic mismatch between the protein and the lipids (Killian, 1998) or more probably in the topographic instabilities that originate from packing defects in the liquid condensed monolayers (Schief et al., 2000), where these defects would allow better protein insertion. Replacing the ethanolamine headgroup by glycerol (DPPG), with negatively charged polar headgroups, resulted in a much lower increase in the surface pressure indicating that the lipid-protein interactions are favored for neutral phospholipids. This is in line with the fact that the protein bears an overall negative charge.

Table. Increases of surface pressure (mN/m) for monolayers of different compositions

DOPE	DPPE	DPPG	DOPE/DPPE (1/1)	DOPE/DPPE (1/1) + Chol (20%)
1.2	6.6	3.0	8.2	9.2

The initial pressure of the monolayers was 23 mN/m with a Cry1Aa concentration of 5×10^{-8} M.

For a mixed monolayer built of DOPE and DPPE (1/1) where the lipids are in phase separation, the surface pressure increase is higher than that observed for the two pure components (*see* Table). This corresponds, as usual, to insertion that is favored by the presence of phase separated domains (Netz, Andelman & Orland, 1996; Dumas et al. 1997; Van Mau et al., 2000).

Since most natural membranes together with those used for single channel experiments, contain cholesterol (CH) we also investigated the influence of CH on the penetration of the protein. The increase of surface pressure induced by the toxin uptake of an equimolecular mixture of DOPE and DPPE was significantly enhanced by the presence of 20% CH (Table). Cry1Aa also significantly raised the surface pressure (from 6 to 14 mN/m) of monomolecular layers made from complex lipid mixtures containing phosphatidylcholine (PC), phosphatidylethanolamine (PE) and CH (5/4/1, mole/mole) that were used to study the electrophysiological characteristics of the pores in black lipid membranes (Schwartz et al., 1993). To avoid these variations in the toxin-induced changes in the surface pressure observed with phospholipids of natural origin likely resulting from variations in the acyl chain composition of PE and PC batches, mixtures of DPPC/DOPE/CH (5/4/1, mole/mole) were used for the rest of the experiments.

To assess whether the toxin can spontaneously insert

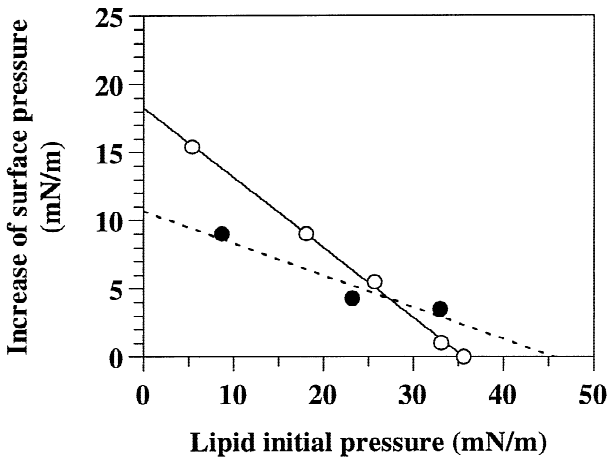

Fig. 2. Variations of the surface pressure of DPPE (continuous line) and DPPC/DOPE/CH (5/4/1, mole/mole) (dashed line) monolayers in the presence of Cry1Aa (concentration = 5×10^{-8} M). The extrapolated critical pressures of insertion are above 35 mN/m. The subphase was maintained at pH 9.34 with 0.1 M sodium carbonate buffer for both cases.

into bilayers, we determined the critical pressure of insertion for two situations. The first one corresponds to a pure phospholipid (DPPE) while the second corresponds to the DPPC/DOPE/CH (5/4/1) mixture. In both cases the critical pressure of insertion (Fig. 2) is higher than 35 mN/m. This value is compatible with a spontaneous insertion of the toxin into bilayers of the above compositions, and thus also probably in biological membranes whose lateral pressure corresponds to a value of approximately 30 mN/m (Demel et al., 1975).

Langmuir-Blodgett Transfers and AFM Observations

Monolayers

The structure of the hydrophobic face of the (PC/PE/CH, 5/4/1) monolayers containing Cry1Aa was examined by AFM after their transfer onto a mica plate using the Langmuir-Blodgett technique. AFM analysis showed the presence of aggregates of an apparent width of 15–100 nm, protruding 1–3 nm from the lipid matrix (Figs. 3*A* and *C*). Since they are exposed to the air and owing to the insertion described above, it is very likely that the protrusions essentially correspond to the most hydrophobic part of the protein. Their width suggests that the toxin is not inserted as single molecules but rather as a group of molecules. Their different heights also suggest that either aggregates can be of different heights or variable degrees of toxin insertion in the monolayer reflecting a nonequilibrium state. However, due to the presence of adhesion forces between the AFM tip and the sample when scanning in air (Shao & Yang, 1995), finer details about the aggregate structure were not obtained. It is worth noting that in absence of toxin, scattered elongated domains up to 400 nm in length protruding from the matrix by ~0.6 nm were imaged (Figs. 3*B* and *D*). Such domains were not observed when Cry1Aa was added, indicating that the toxin interfered with their formation. Considering the lipid composition, it seems reasonable to assume that the domains correspond to either liquid-condensed or liquid-ordered cholesterol- enriched regions of the monolayer (Silvius, del Guidice & Lafleur, 1996).

Bilayers

We next examined the carbonate buffer-membrane interface of asymmetrical supported lipid bilayers by AFM where the leaflet accessible to the toxin was made of PC/PE/CH mixtures and the leaflet facing the mica was composed of dipalmitoylphosphatidylcholine (DPPC). This procedure of bilayer formation is similar to the ⟨⟨tip-dip⟩⟩ technique that has been used to measure the electrophysiological properties of active channels in lipid bilayers (Mak & Webb, 1995; Henry et al., 1996; Thrower, Lea & Dawson, 1998). The transfer surface pressure of the second monolayer with the toxin inserted, was close to 30 mN/m. It is known that the use of surface pressures above 15 mN/m prevents the unfolding of membrane proteins at the interface and maintains their activity in monolayers (Pattus et al., 1981). AFM imaging was conducted on the hydrophilic side of the external leaflet which, with respect to biological membranes, would correspond to the external leaflet of a cell membrane. Low magnification images showed protein aggregates of 30–100 nm in diameter rising up to ~3 nm from the bilayer surface (Fig. 4*A*), which were absent at the surface of control bilayers in the absence of toxin (Fig. 4*B*). The width of the aggregates at the membrane-solution interface was in the range of that observed for the hydrophobic face of the monolayers (Fig. 3*A*). The well-defined phase-separated domains visualized on the hydrophobic side of control monolayers (Fig. 3*B*) were not seen when imaging the hydrophobic side of the control bilayer. This suggests that the longest aliphatic tails of DPPC/DOPE/CH monolayers can intercalate the aliphatic tails of the DPPC monolayer facing the mica; 500-nm scans (Fig. 4*C*) revealed small structures showing a central depression, not observed in controls at identical magnification (Fig. 4*D*). These structures were primarily localized at the periphery of aggregates (black arrows) but some appeared isolated (white arrows) in the lipid bilayer. Two successive scans of the same area at the edge of an aggregate confirmed the reproducibility of

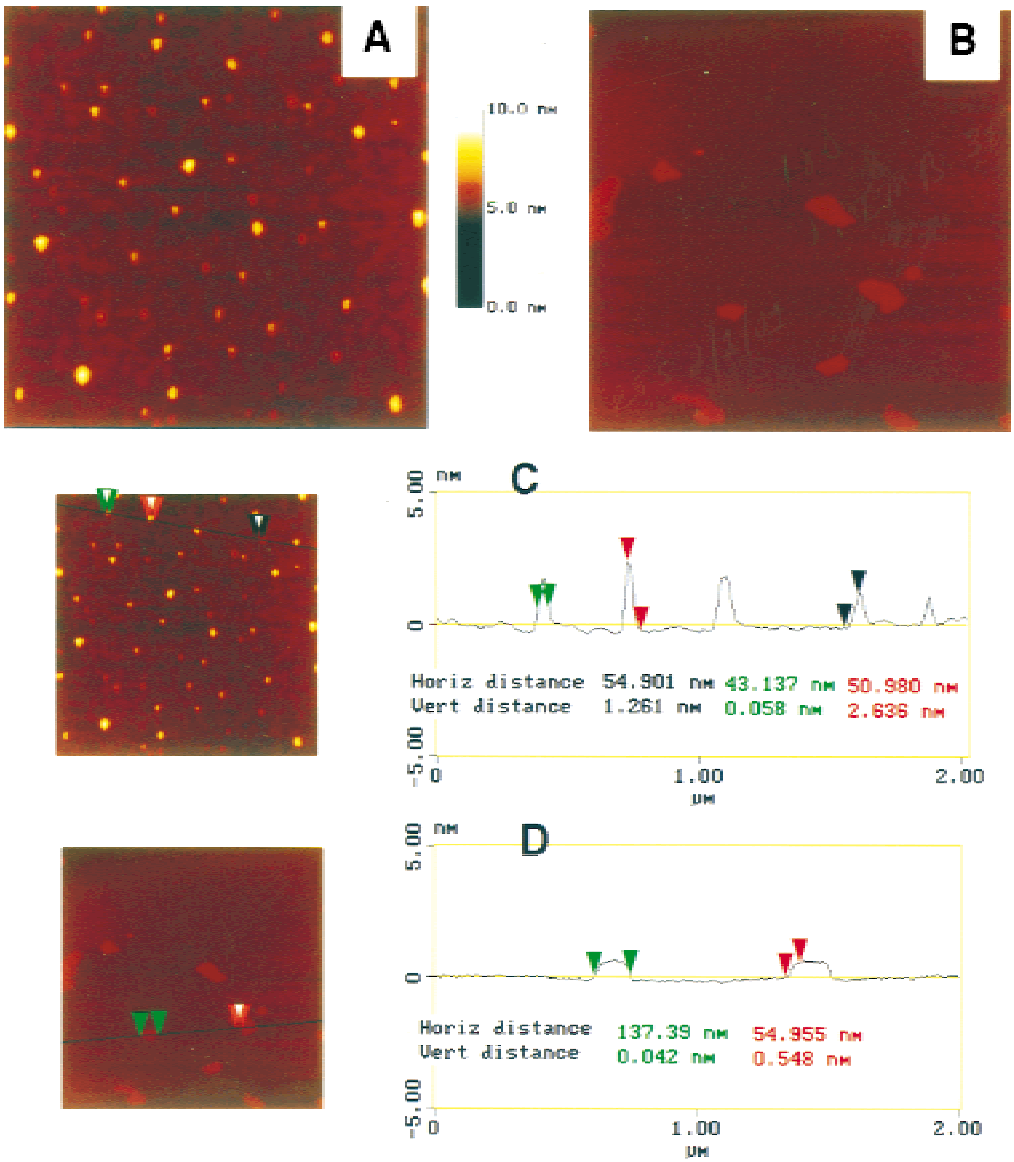

Fig. 3. Atomic force microscopy image of the air-exposed face of a Langmuir-Blodgett film with inserted Cry1Aa. The monolayer made of DPPC/DOPE/CH (5/4/1, mole/mole) was compressed to 24 mN/m before the addition of Cry1Aa (5×10^{-8} M) into the subphase. The film was transferred onto the mica once the surface pressure attained 30 mN/m, and its hydrophobic face examined in air (Fig. 3*A*). This top view of the surface shows the presence of aggregates protruding up to ~3 nm above the methyl end of phospholipids (Fig. 3*C*). Controls transferred at the same surface pressure, in the absence of toxin, show the presence of lipid domains (Fig. 3*B*) protruding ~0.5 nm from the matrix (Fig. 3*D*).

the imaging and are presented in Figs. 4*E* and *F*. Identical porelike structures of an apparent diameter of 5 nm and protruding 0.5–0.6 nm above the matrix are clearly visible on both images (Figs. 4*E* and *F*). At higher magnification (Fig. 4*G*), the particles appear to possess four subunits of 1.4 nm diameter each, surrounding a depression of 1.5 nm in diameter (arrow). Similar structures apparently protruding up to 2 nm above the lipid matrix were observed in the aggregates although less resolved (Fig. 4*G*). They most likely resulted from local deformation of the bilayer induced by the aggregates. This high level of lateral resolution, which was previously achieved only with 2-D crystals of membrane proteins, was probably a consequence of aggregate formation exerting a stabilizing influence on the pore and of the use of DPPC as the second membrane leaflet to limit lateral diffusion of the protein in the bilayer (Müller, Büldt & Engel, 1995; Mou, Yang & Shao, 1995; Heymann et al. 1997). Such a feature is in agreement with the pore model previously reported (Masson et al. 1999).

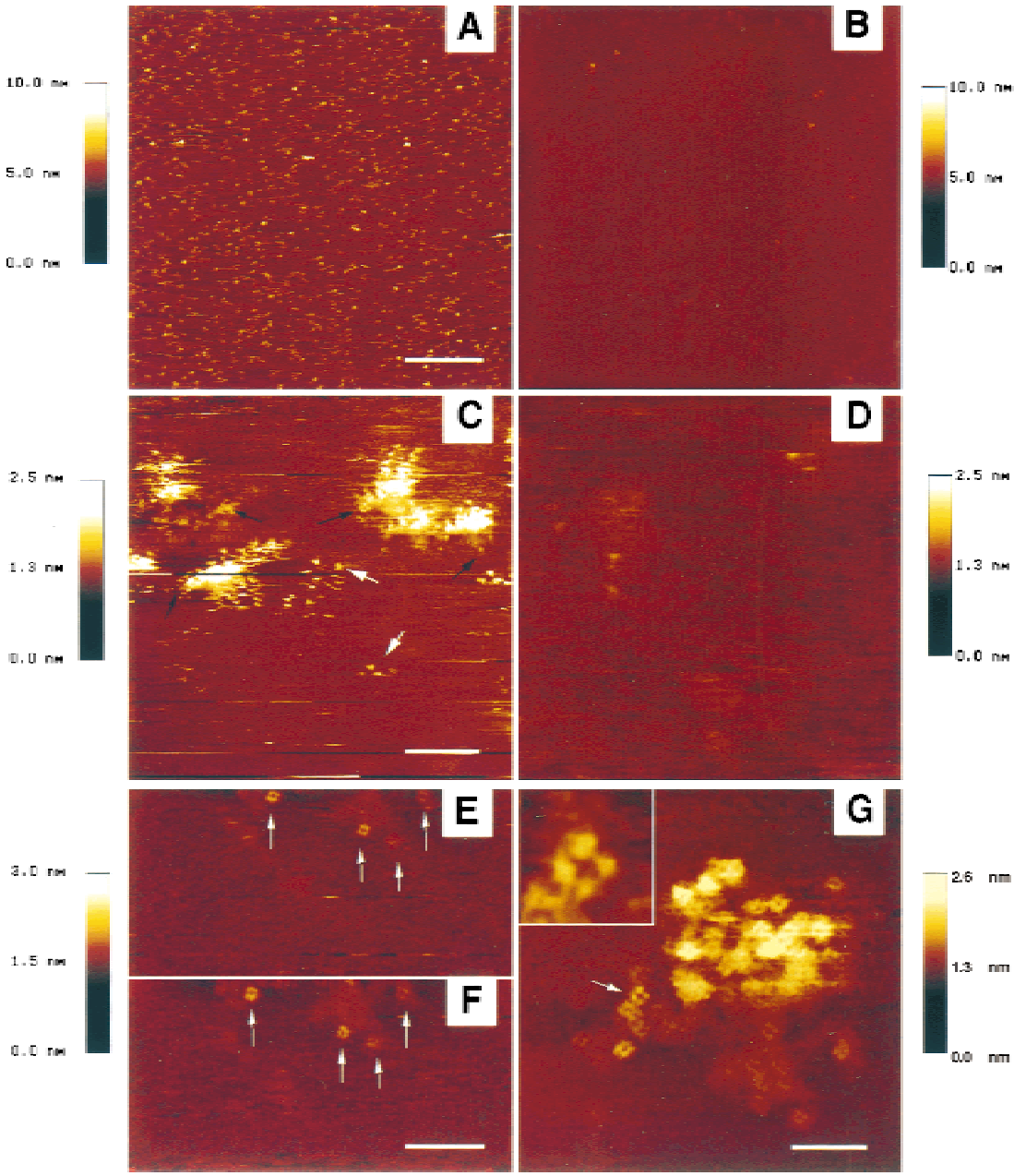

Fig. 4. Atomic force microscopy imaging of lipid bilayers with inserted Cry1Aa. *A, C, E, F* and *G* correspond to bilayers containing inserted Cry1Aa imaged under carbonate buffer. *B* and *D* are images of control bilayers, without toxin, at magnifications identical to *A* and *C*, respectively. Bar sizes (white) are 1000, 100, 30 and 20 nm in size for panels *A, C, E* and *G*, respectively. Size of the inset in panel *G* containing the single pore: 10 × 10 nm. The different height scales are shown beside each panel.

FTIR Investigations

For a better understanding of the mechanism of insertion of the protein in membranes and to examine possible conformational changes suggested by the existence of an anisotropic interface, at least concerning the secondary structure, we undertook FTIR investigations of Cry1Aa in the absence, i.e., in solution, or in the presence of the lipid mixture used for the Langmuir-Blodgett transfers. This spectroscopic approach is more appropriate than CD, for example, for investigating variations of the secondary structure of a protein when varying its environ-

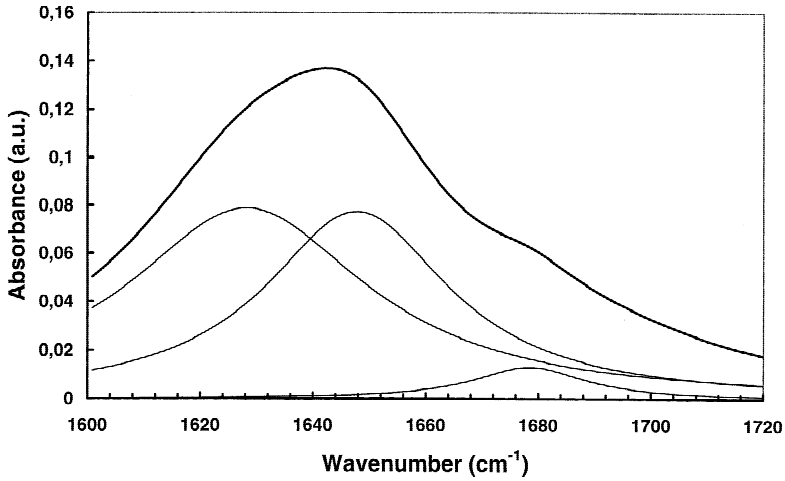

Fig. 5. FTIR spectrum of Cry lAa solution in 0.1 M sodium carbonate buffer. The heavy line corresponds to the crude spectrum obtained by subtracting the spectrum of the buffer from that of the protein in solution in the buffer. The other spectra are the results from the decomposition process.

ment, especially when going from a homogeneous one (a solution) to a lipid-containing environment that is generally more heterogeneous. The spectra of the Amide I band region for both conditions are shown in Figs. 5 and 6, respectively. For the protein in the carbonate or Tris buffer solution, the Amide I band was characterized by a broad band centered around 1640 cm^{-1}, which could be decomposed into two major contributions of about the same intensity, and which lie at 1627 and 1650 cm^{-1} (Fig. 5). These two bands can be attributed to β-type and α-helical structures, respectively (Arrondo et al., 1993; Tamm & Tatulian, 1997). In addition, the presence of a shoulder at 1680 cm^{-1} suggests an antiparallel arrangement of the β-strands (Dong, Huang & Caughey, 1990). This analysis is consistent with the known atomic structure of Cry1Aa. Note that the same spectrum was obtained for the protein in the solid state, i.e., when the water was allowed to evaporate.

The presence of lipid (DPPG or the DPPC/DOPE/CH; 5/4/1 mixture) induced drastic modifications of the spectrum characterized by a shift of the Amide I band to 1656 cm^{-1} (Fig. 6), indicating that upon insertion into lipid media, the protein undergoes important conformational changes. Note that the band attributed to the phospholipids, which lies around 1735 cm^{-1}, remains almost unchanged (Fig. 6*A*). The curve-fitting procedure shows that the low wavenumber contribution at 1627 cm^{-1} almost disappears for the benefit of an Amide I band lying around 1673 cm^{-1} while that lying around 1650 cm^{-1} remains almost unchanged with, however, a small shift down to 1646 cm^{-1} (Fig. 6*B*). This strongly suggests that upon binding to lipids, an unfolding of the β-type structures occurs, similar to that previously reported for Cyt toxins. Further, the shift of the helical contribution could be indicative of helical associations (Heimburg et al., 1996).

Conclusion

The present study establishes that spontaneous insertion of Cry1Aa in receptor-free lipid bilayers results in the formation of porelike structures, most often aggregated. The fact that Cry1Aa can insert into lipid bilayers in the absence of receptor is in agreement with previous reports based on electrophysiological studies. The observation that insertion can occur in lipid monolayers depending on the lipid composition and/or physical state, implies that the large reorganization required to evolve from a soluble to a membrane-bound and finally to the inserted state is determined by the interfacial properties of the external leaflet of the bilayer. The examination of the hydrophobic side of the monolayer reveals large aggregates emerging in the air, i.e., a hydrophobic environment, with a height that can exceed the thickness of a membrane leaflet. This indicates that following the interaction with the solution-membrane interface, a large part of the toxin reorganizes to expose a hydrophobic surface to the environment. Considering the structure of the soluble form of the toxin, this insertion must involve large structural rearrangements, a view that is supported by earlier works (Schwartz et al., 1997; Masson at al., 1999) and now by the FTIR data.

The porelike structure exposed at the buffer-bilayer interface appears to be formed by the association of four subunits whose dimensions, as estimated by AFM, are consistent with single α-helical structures. Owing to the experimental conditions, especially with regard to the protein concentration used for the insertion before transfer, it is likely that the pore formation results from a tetrameric association of toxin molecules. Both the size and structure of the pore are in accordance with the recent model for Cry1Aa insertion in membrane. On the other hand, one can only speculate about the localization of the remaining part of the toxin molecule with regard to

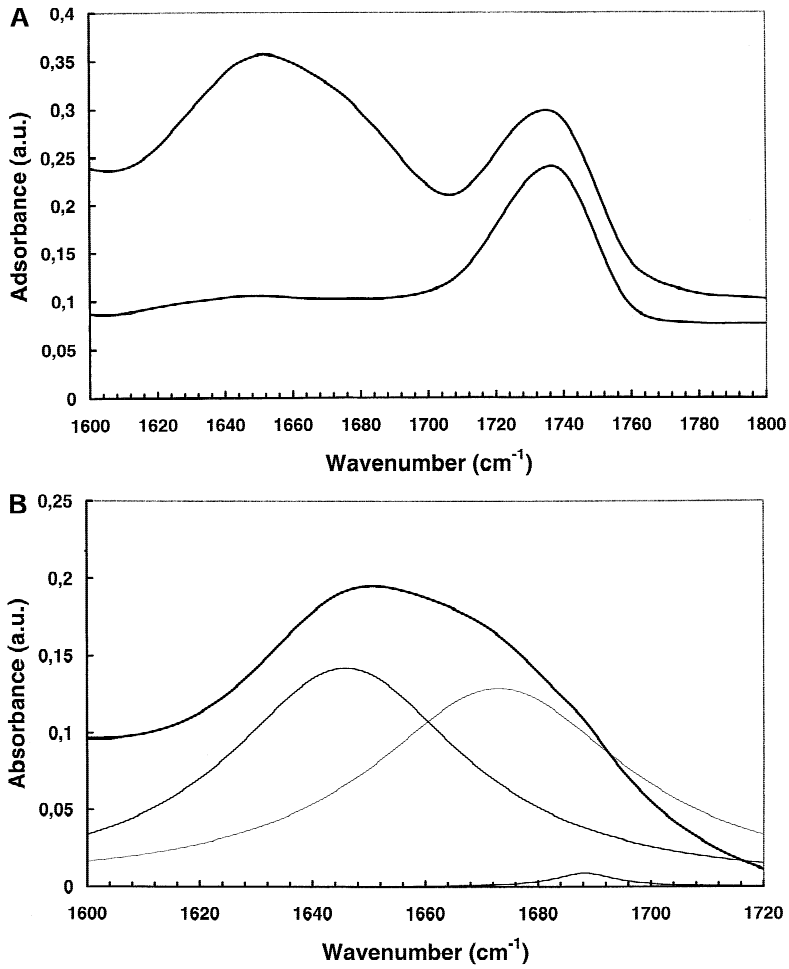

Fig. 6. FTIR spectra of Cry1Aa in the presence of phospholipids. (*A*) Upper spectrum: mixture of DPPC/DOPE/CH (5/4/1, mole/mole) without protein. Lower spectrum: mixture of PC/PE/CH (5/4/1, mole/mole) containing the protein. (*B*) (Result of the subtraction between the two spectra of *A* to show only the Amide I band contribution (heavy line). The other spectra correspond to the decomposition in order to show the various conformational contributions.

the bilayer. The model proposed earlier for the Bt toxin pore was derived from black lipid membrane experiments in which the protein insertion was realized after the bilayer has been formed. On the contrary, for the experiments reported here the protein was incorporated into the lipid monolayer prior to transfer. This difference in experimental protocols may account for the fact that the AFM images do not support a localization where the major part of the toxin lies at the buffer-bilayer interface. In addition, surface pressure measurements, AFM and FTIR data obtained in receptor-free membranes suggest that a large part of the toxin is embedded within the lipid bilayer and thus not observable by AFM when examined from the polar side. This is consistent with the unfolding of the protein when interacting with lipids and with being generally accompanied by the formation of hydrophobic domains that are able to interact with the hydrophobic environment of a bilayer and is in agreement with previous observations indicating that, when bound to vesicles, Cry1Ac was largely resistant to digestion with protease K (Aronson, Geng & Wu, 1999).

This work was supported by the GDR N° 790 from the CNRS. We are grateful to Dr. P. Bello for manuscript corrections.

References

Arrondo, J.L.R., Muga, A., Castresana, J., Goni, F.M. 1993. Quantitative studies of the structure of proteins in solution by Fourier transform infrared spectroscopy. *Prog. Biophys. Mol. Biol.* **59:**23–56

Aronson, A.I., Geng, C., Wu, L. 1999. Aggregation of *Bacillus thuringiensis* Cry1A toxins upon binding to target insect larval midgut vesicles. *Appl. Environ. Microbiol.* **65:**2503–2507

Brockman, H. 1999. Lipid monolayers: why use half a membrane to characterize protein-membrane interactions? *Curr. Opin. Struct. Biol.* **9:**438–443

Bradford, M.M. 1976. A rapid and sensitive method for the quantitation of microgram quantities of protein utilizing the principle of protein-dye binding. *Anal. Biochem.* **72:**248–254.

Demel, R.A., Geurts van Kessel, W.S., Zwaal, R.F., Roelofsen, B., van Deenen, L.L. 1975. Relation between various phospholipase actions on human red cell membranes and the interfacial phospholipid pressure in monolayers. *Biochim. Biophys. Acta* **406:**97–107

Dong, A., Huang, P., Caughey, W.S. 1990. Protein secondary structures in water from second-derivative amide I infrared spectra. *Biochemistry* **29:**3303–3308

Dumas, F., Sperotto, M.M., Lebrun, M-C., Tocanne, J-F., Mouritsen, O.G. 1997. Molecular sorting of lipids by bacteriorhodopsin in dilauroylphosphatidylcholine/distearoyl phosphatidylcholine lipid bilayers. *Biophys. J.* **73:**1940–1953

Gazit, E., Shai, Y. 1995. The assembly and organization of the alpha 5

and alpha 7 helices from the pore-forming domain of *Bacillus thuringiensis* delta-endotoxin. Relevance to a functional model. *J. Biol. Chem.* **270:**2571–-2578

Gazit, E., LaRocca, P., Sansom, M.S P., Shai, Y. 1998. The structure and organization within the membrane of the helices composing the pore-forming domain of *Bacillus thuringiensis* delta-endotoxin are consistent with an "umbrellalike" structure of the pore. *Proc. Natl. Acad. Sci. USA* **95:**12289–12294

Green, R.J., Hopkinson, I., Jones, R.A.L. 1999. Unfolding and intermolecular association in globular proteins adsorbed at interfaces. *Langmuir* **15:**5102–5110

Grochulski, P., Masson, L., Borisova, S., Pusztai-Carey, M., Schwartz, J.L., Brousseau, R., Cygler, M. 1995. *Bacillus thuringiensis* CryIA(a) insecticidal toxin: crystal structure and channel formation. *J. Mol. Biol.* **254:**447–464

Güereca, L., Bravo A. 1999. The oligomeric state of *Bacillus thuringiensis* Cry toxins in solution. *Biochim. Biophys. Acta* **1429:**342–350

Heimburg, T., Schuenemann, J., Weber, K., Geisler, N. 1996. Specific recognition of coiled coils by infrared spectroscopy: analysis of the three structural domains of Type III intermediate filament proteins. *Biochemistry* **35:**1375–1382

Henry, J.P., Juin, P., Valette, F., Thieffry, M. 1996. Characterization and function of the mitochondrial outer membrane peptide-sensitive channel. *J. Bioenerg. Biomembr.* **28:**101–108

Heymann, J.B., Müller, D.J., Mitsuoka, K., Engel, A. 1997. Electron and atomic force microscopy of membrane proteins. *Curr. Opin. Struct. Biol.* **7:**543–549

Killian, J.A. 1998. Hydrophobic mismatch between proteins and lipids in membranes. *Biochim. Biophys. Acta* **1376:**401–415

Le Grimellec, C., Lesniewska, E., Cachia, C., Schreiber, J.P., de Fornel, F., Goudonnet, J.P. 1994. Imaging of the membrane surface of MDCK cells by atomic force microscopy. *Biophys. J.* **67:**36–41

Le Grimellec, C., Lesniewska, E., Giocondi, M.C., Finot, E., Vie, V., Goudonnet, J.P. 1998. Imaging of the surface of living cells by low-force contact-mode atomic force microscopy. *Biophys. J.* **75:**695–703

Losey, J.E., Rayor, L.S., Carter, M.E. 1999. Transgenic pollen harms monarch larvae. *Nature* **399:**214

Mak, D.O., Webb, W.W. 1995. Two classes of alamethicin transmembrane channels: molecular models from single-channel properties. *Biophys. J.* **69:**2323–2336

Masson, L., Tabashnik, B.E., Liu, Y.B., Brousseau, R., Schwartz, J.L. 1999. Helix 4 of the *Bacillus thuringiensis* Cry1Aa toxin lines the lumen of the ion channel. *J. Biol. Chem.* **274:**31996–32000

Mou, J., Yang, J., Shao, Z. 1995. Atomic force microscopy of cholera toxin B-oligomers bound to bilayers of biologically relevant lipids. *J. Mol. Biol.* **248:**507–512

Müller, D.J., Büldt, G., Engel, A. 1995. Force-induced conformational change of bacteriorhodopsin. *J. Mod. Biol.* **249:**239–243

Netz, R.R., Andelman, D., Orland, H. 1996. Protein adsorption on lipid monolayers at their coexistence region. *J. Phys. II* **6:**1023–1047

Pattus, F., Rothen, C., Streit, M., Zahler, P. 1981. Structure, composition, enzymatic activities of human erythrocyte and sarcoplasmic reticulum membrane films. *Biochim. Biophys. Acta* **647:**29–39

Rafalski, M., Lear, J.D., DeGrado, W.F. 1990. Phospholipid interactions of synthetic peptides representing the N-terminus of HIV gp41. *Biochemistry* **29:**7917–7922

Rang, C., Vachon, V., de Maagd, R.A., Villalon, M., Schwartz, J.L., Bosch, D., Frutos, R., Laprade, R. 1999. Interaction between functional domains of *Bacillus thuringiensis* insecticidal crystal proteins. *Appl. Environ. Microbiol.* **65:**2918–2925

Schief, W.R., Touryan, L., Hall, S.B., Vogel, V. 2000. Nanoscale topographic instabilities of a phospholipid monolayer. *J. Phys. Chem. B.* **104:**7388–7393

Schnepf, E., Crickmore, N., Van Rie, J., Lereclus, D., Baum, J., Feitelson, J., Zeigler, D.R., Dean, D.H. 1998. *Bacillus thuringiensis* and its pesticidal crystal proteins. *Microbiol. Mol. Biol. Rev.* **62:**775–806

Schwartz, J.L., Garneau, L., Savaria, D., Masson, L., Brousseau, R., Rousseau, E. 1993. Lepidopteran-specific crystal toxins from *Bacillus thuringiensis* form cation- and anion-selective channels in planar lipid bilayers. *J. Membrane Biol.* **132:**53–62

Schwartz, J.L., Juteau, M., Grochulski, P., Cygler, M., Prefontaine, G., Brousseau, R., Masson, L. 1997. Restriction of intramolecular movements within the Cry1Aa toxin molecule of *Bacillus thuringiensis* through disulfide bond engineering. *FEBS Lett.* **410:**397–402

Shao, Z., Yang, J. 1995. Progress in high resolution atomic force microscopy in biology. *Q. Rev. Biophys.* **28:**195–251

Silvius, J.R., del Guidice, D., Lafleur, M. 1996. Cholesterol at different bilayer concentrations can promote or antagonize lateral segregation of phospholipids of differing acyl chain length. *Biochemistry* **35:**6197-6202

Tabashnik, B.E., Liu, Y.B., Malvar, T., Heckel, D.G., Masson, L., Ballester, V., Granero, F., Mensua, J.L., Ferre, J. 1997. Global variation in the genetic and biochemical basis of diamondback moth resistance to *Bacillus thuringiensis. Proc. Nad. Acad. Sci. USA* **94:**12780–12785

Tamm, L.K., Tatulian, S.A. 1997. Infrared spectroscopy of proteins and peptides in lipid bilayers. *Q. Rev. Biophys.* **30:**365–429

Thrower, E.C., Lea, E.J., Dawson, A.P. 1998. The effects of free [Ca^{2+}] on the cytosolic face of the inositol (1,4,5)-trisphosphate receptor at the single channel level. *Biochem. J.* **330:**559–564

Van Mau, N., Vié, V., Chaloin, L., Lesniewska, E., Heitz, F., Le Grimellec, C. 1999. Lipid-induced organization of a primary amphipathic peptide: a coupled AFM-monolayer study. *J. Membrane. Biol.* **167:**241–249

Van Mau, N., Misse, D., Le Grimellec, C., Divita, G., Heitz, F., Veas, F. 2000. The SU glycoprotein 120 from HIV-1 penetrates into lipid monolayers mimicking plasma membranes. *J. Membrane Biol.* **177:**251–257

Vié, V., Van Mau, N., Lesniewska, E., Goudonnet, J.P., Heitz, F., Le Grimellec, C. 1998. Distribution of ganglioside G_{M1} between two-components, two-phase phosphatidylcholine monolayers. *Langmuir* **14:**4574–4583